

## Toward the Spectrum of Free Polyethylene: Linear Alkanes Studied by Carbon 1s Photoelectron Spectroscopy and Theory

Tor Karlsen,<sup>\*,†</sup> Knut J. Børve,<sup>†</sup> Leif J. Sæthre,<sup>†</sup> Karoline Wiesner,<sup>‡</sup>  
Margit Bässler,<sup>‡</sup> and Svante Svensson<sup>‡</sup>

*Contribution from the Department of Chemistry, University of Bergen, N-5007 Bergen, Norway,  
and Department of Physics, Uppsala University, Box 530, S-75121 Uppsala, Sweden*

Received March 12, 2001

**Abstract:** Trends in carbon 1s ionization energies for the linear alkanes have been investigated using third-generation synchrotron radiation. The study comprises CH<sub>4</sub>, C<sub>2</sub>H<sub>6</sub>, C<sub>3</sub>H<sub>8</sub>, C<sub>4</sub>H<sub>10</sub>, C<sub>5</sub>H<sub>12</sub>, C<sub>6</sub>H<sub>14</sub>, and C<sub>8</sub>H<sub>18</sub>. Both inter- and intramolecular shifts in ionization energy have been determined from gas-phase spectra and ab initio calculations. The shifts are decomposed into initial-state and final-state contributions and are shown to relate to the fundamental chemical properties of group electronegativity and polarizability. By extrapolation, we predict C1s spectra of larger *n*-alkanes, converging toward isolated strands of polyethylene.

### 1. Introduction

Chemical properties such as acidity, proton affinity, and reactivity toward electrophilic reagents are related to the molecular charge distribution and its ability to reorganize upon local perturbations. To understand and predict the outcome of such reactions, it is useful to study the underlying electronic properties, to which end X-ray photoelectron spectroscopy (XPS) is an excellent technique. First, core electrons are largely localized to specific atoms. Second, the binding energy of inner-shell electrons depends on the charge distribution in the molecule and the ability of the neighboring atoms to screen the positive charge introduced through ionization. Hence, core-ionization energies express the ability of a molecule to accept charge at a specific site. Third, state-of-the-art synchrotrons facilitate inner-shell photoelectron spectra with an energy resolution much higher than the width defined by the lifetime of the core hole. In the case of C1s ionization, this means a combined instrumental and lifetime broadening just above 0.1 eV, and combined with deconvolution methods, XPS spectra can provide energy shifts of chemical accuracy (1 kcal/mol  $\approx$  0.05 eV).

The alkane series is well suited for investigating how the electronic properties develop within a saturated molecular system of increasing size, in that these molecules show substantial vapor pressure at experimental conditions for a considerable number of carbon atoms. The observed spectrum for each *n*-alkane may be regarded as a superposition of subspectra originating from ionization of each symmetry-unique carbon atom in the molecule. With a priori knowledge of the line shape of each subspectrum, intramolecular chemical shifts

may be obtained from least-squares fits to the recorded spectra. The subspectra have asymmetric line shapes caused by the decay process of the hole states and, more importantly, because of vibrational excitation of the ion. We have recently described a computational procedure for obtaining such site-specific line shapes on the basis of ab initio calculations.<sup>1</sup> Such calculations have been shown to provide accurate representations of the line shapes in C1s photoelectron spectra of ethane<sup>2</sup> and other hydrocarbons.<sup>3</sup>

A rather extensive study of trends in C1s ionization energies was performed by Pireaux et al.<sup>4</sup> Using conventional Al K $\alpha$  X-rays, they found the ionization energies to range over 0.6 eV among the first 13 *n*-alkanes, decreasing with increasing molecular size. From calculations, it was concluded that the observed shifts in ionization energy ( $\Delta I$ ) were largely determined by electronic relaxation. With the instrumental resolution available at that time, the reported  $\Delta I$ 's represent average ionization energies of the carbon atoms present in each molecule. However, technological advances allow us to resolve for the first time also intramolecular shifts for a number of linear alkanes, in addition to intermolecular shifts of unprecedented accuracy.

Further insight may be obtained by separating the ionization energy of a particular site into a contribution *V* pertaining to the charge distribution in the neutral molecule, and a contribution *R* because of electronic and geometric relaxation in the ionized molecule, according to<sup>5</sup>

- (1) Karlsen, T.; Børve, K. *J. J. Chem. Phys.* **2000**, *112*, 7979.
- (2) Karlsen, T.; Sæthre, L. J.; Børve, K. J.; Berrah, N.; Kukk, E.; Bozek, J. D.; Carroll, T. X.; Thomas, T. D. *J. Phys. Chem. A* **2001**, *105*, 7700.
- (3) Sæthre, L. J.; Berrah, N.; Bozek, J. D.; Børve, K. J.; Carroll, T. X.; Kukk, E.; Gard, G. L.; Winters, R.; Thomas, T. D. *J. Am. Chem. Soc.* **2001**, *123*, 10729.
- (4) Pireaux, J. J.; Svensson, S.; Basilier, E.; Malmqvist, P.-Å.; Gelius, U.; Caudano, R.; Siegbahn, K. *Phys. Rev. A* **1976**, *14*, 2133.

\* To whom correspondence should be addressed. E-mail: tor.karlsen@hydro.com.

<sup>†</sup> University of Bergen.

<sup>‡</sup> Uppsala University.

$$I = V - R \quad (1)$$

To a first approximation,  $V$  is determined by the electrostatic potential at the site of ionization (multiplied by a unit positive charge to convert from potential to potential energy). To take into account both the wave nature of core electrons and the influence of valence-electron correlation on the electrostatic potential, Børve and Thomas<sup>6</sup> developed the following expression for a shift in the initial-state contribution:

$$\Delta V \approx \Delta U^{\text{VCI}} - (\Delta \epsilon_c + \Delta U^{\text{HF}}) \quad (2)$$

$\Delta \epsilon_c$  is the difference in initial-state core-orbital energies, and  $\Delta U$  is the difference in electrostatic energy of a unit positive charge at the two nuclei that are being compared. Superscripts HF and VCI denote Hartree–Fock and valence-correlated levels of theory, respectively. Equation 2 is valid in the case of well-localized or close-to-degenerate inner-shell orbitals.

Generation of a core hole induces both intra- and extra-atomic electronic relaxation effects. The former is dominated by contraction of valence orbitals toward the core hole and is expected to be fairly constant within the alkane series. The second and more important contribution to  $\Delta R$  reflects the screening of the core hole by means of electron transfer and polarization of the substituents at the ionized atom. This part measures how readily the electron distribution of a group adapts to a change in the electrostatic field set up by its surroundings. Shifts in the electronic relaxation energy,  $\Delta R$ , can be estimated by different approaches (see, e.g., ref 5); here, we combine the experimental values for  $\Delta I$  with  $\Delta V$  computed according to eq 2, to obtain  $\Delta R = \Delta V(\text{calc}) - \Delta I(\text{exp})$ .

In the present study, we have measured the C1s photoelectron spectra of CH<sub>4</sub>, C<sub>3</sub>H<sub>8</sub>, C<sub>4</sub>H<sub>10</sub>, C<sub>5</sub>H<sub>12</sub>, C<sub>6</sub>H<sub>14</sub>, and C<sub>8</sub>H<sub>18</sub> using third-generation synchrotron radiation. The extracted shifts in ionization energy are resolved into initial- and final-state contributions, and their dependence on the position of the carbon atoms and the size of the molecules is used to explore the electronic properties of alkyl moieties in general. Our findings confirm the notion of methyl groups as being electron withdrawing when engaged in saturated hydrocarbons,<sup>7</sup> contrary to their donating nature when bonded to unsaturated groups.<sup>3</sup>

In addition to forming a prominent class of compounds in their own right, the linear alkanes are interesting in that they converge to polyethylene. Polyethylene exists in crystalline or amorphous forms, and the C1s spectra undergo additional broadening because of intermolecular interference, effectively making it impossible to extract the spectrum of a single strand of polymer from the solid-state spectra. On the other hand, access to such a single-strand spectrum is potentially useful for comparison with spectra of solid-state samples. Earlier attempts<sup>8,9</sup> to explain the asymmetry of the C1s line in solid-state polyethylene have relied on an analogy to the gas-phase spectrum of methane.<sup>10</sup> Here, we construct a highly resolved

molecular spectrum of polyethylene by extrapolation of site-specific C1s ionization data for  $n$ -alkanes.

## 2. Experimental Section

Carbon 1s photoelectron spectra were acquired at beamline I411<sup>11</sup> at the MAX-2 laboratory in Lund, Sweden. The measurements were made using a photon energy of 330 eV. This is some 39 eV above the ionization threshold, and the interaction between electrons from the Auger decay process and the outgoing photoelectron (postcollision interaction, or PCI) is relatively weak. The energy scale of each spectrum was calibrated by mixing the sample gas with CO<sub>2</sub> and measuring the two C1s spectra simultaneously. In the calibration, the adiabatic ionization energy of CO<sub>2</sub> (297.664 eV) was taken from ref 12. The spectrometer was aligned at an angle of 54.7° to the electric-field vector of the light and at 90° to its propagation direction. Beamline I411 receives its radiation from a 58.8-mm-period undulator and a Zeiss SX-700 plane grating monochromator that is, in principle, capable of a resolving power ( $E/\Delta E$ ) of about 6000 (at a photon energy of 400 eV). The kinetic energy of the photoelectrons was analyzed using a Scienta SES-200 hemispherical electron energy analyzer.

The measurements were performed during three different periods (May, June, and September 1999), with similar beamline settings and instrumental resolution. The instrumental contribution to the total line width was determined to be about 65 meV (fwhm) from the C1s spectrum of methane, for which the Lorentzian width has been determined to be 95(5) meV.<sup>13</sup>

Methane (99.95%), propane (99.5%),  $n$ -butane (99.5%),  $n$ -pentane (99%),  $n$ -hexane (99%), and  $n$ -octane (99%) were obtained from commercial sources. The gases were introduced into the inlet system without further purification. Data acquisitions were made as series of short runs, with the data from each run being inspected and the energy scale adjusted to account for small drifts in energy.

## 3. Models Used in the Analysis of the Spectra

In a linear C <sub>$n$</sub> H<sub>2 $n$ +2</sub> alkane, there are  $n/2$  ( $n$  even) or  $(n + 1)/2$  ( $n$  odd) symmetry-unique carbon atoms that provide individual contributions to the C1s spectrum. Hence, the observable spectrum is a superposition of site-specific subspectra, each of which are broadened into a site-specific line shape by vibrational excitation in the core-ionized molecule. In this work, site-specific vibrational profiles have been generated in the Franck–Condon approximation as described in ref 14, employing equilibrium geometries, normal modes, and vibrational energies for the ground and core-ionized states as obtained in density functional (DFT) calculations; see Appendix for details. Each profile is named according to the position of the corresponding carbon atom numbered from the end of the molecule; that is, C1 corresponds to methyl carbons in all compounds.

The experimental spectra were analyzed by fitting the theoretical profiles to the spectra using least-squares techniques.<sup>15</sup> Relative intensities of the site-specific profiles were restricted to ratios in total area given by stoichiometry; the only fitting parameters were constant background, overall intensity, and position of the lines. Each vibrational line in the spectrum

(5) Thomas, T. D. *J. Electron Spectrosc. Relat. Phenom.* **1980**, *20*, 117.  
 (6) Børve, K. J.; Thomas, T. D. *J. Electron Spectrosc. Relat. Phenom.* **2000**, *107*, 155.  
 (7) Tasi, G.; Mizukami, F.; Pálinkó, I. *J. Mol. Struct.* **1997**, *401*, 21.  
 (8) Beamson, G.; Clark, D. T.; Kendrick, J.; Briggs, D. *J. Electron Spectrosc. Relat. Phenom.* **1991**, *57*, 79.  
 (9) Beamson, G.; Briggs, D. *High-Resolution XPS of Organic Polymers: The Scienta ESCA 300 Database*; Wiley: Chichester, 1992.  
 (10) Gelius, U.; Svensson, S.; Siegbahn, H.; Basilièr, E.; Faxälv, Å.; Siegbahn, K. *Chem. Phys. Lett.* **1974**, *28*, 1.

(11) Bässler, M.; Ausmees, A.; Jurvansuu, M.; Feifel, R.; Forsell, J.-O.; Fonseca, P.; Kivimäki, A.; Sundin, S.; Sorensen, S. L.; Nyholm, R.; Björneholm, O.; Aksela, S.; Svensson, S. *Nucl. Instrum. Methods A* **2001**, *469*, 382.  
 (12) Myrseth, V.; Bozek, J. D.; Kukk, E.; Sæthre, L. J.; Thomas, T. D. *J. Electron Spectrosc. Relat. Phenom.* **2002**, *122*, 57.  
 (13) Carroll, T. X.; Berrah, N.; Bozek, J.; Hahne, J.; Kukk, E.; Sæthre, L. J.; Thomas, T. D. *Phys. Rev. A* **1999**, *59*, 3386.  
 (14) Thomas, T. D.; Sæthre, L. J.; Sorensen, S. L.; Svensson, S. *J. Chem. Phys.* **1998**, *109*, 1041.  
 (15) Kukk, E. *SPANCF 2000*; — <http://www.geocities.com/ekukk>, 2000.

was broadened to a line shape that includes instrumental resolution, lifetime broadening, and interaction between photoelectrons and the faster Auger electrons (PCI). To model the effect of PCI, we have used the approach by van der Straten et al.,<sup>16</sup> with a Lorentzian lifetime width of 100 meV<sup>2</sup> and a Gaussian width of 65 meV for the instrumental resolution. The PCI effect is included in the line shape as defined from an asymmetry parameter of  $1/\sqrt{2E_P} - 1/\sqrt{2E_A}$ , where  $E_P$  is the kinetic energy of the photoelectron, and  $E_A$  is the kinetic energy of the Auger electron (in au). The Auger spectra of the compounds under investigation all have their most pronounced feature at 249 eV,<sup>17</sup> corresponding to an asymmetry parameter of 0.36.

Adiabatic ionization energies ( $I$ ) are directly available from the fitting procedure as outlined, whereas vertical ionization energies are obtained as centers of gravity of the vibrational profiles. These profiles are based on all vibrational lines that receive more than 0.1% of the total intensity associated with each carbon atom. For the larger molecules, this criterion implies the neglect of a large number of very weak vibrational lines, and for this reason, the vertical energies are associated with larger uncertainties than is the corresponding  $I$ . For this reason, our shift analysis is based on adiabatic energies, implying that the associated relaxation energies ( $R$ ) include contributions from electronic as well as geometric relaxation of the molecule. Within the harmonic-oscillator approximation, the mean vibrational excitation energy is computed to 0.16 eV in core-ionized methane and increases slowly with chain length from 0.18 eV in ethane to 0.20 eV in *n*-octane. From these numbers, geometric relaxation contributes only 0.02–0.04 eV to  $\Delta R$  computed relative to methane.

The computational models were restricted to the all-trans conformers, even though the number of thermodynamically accessible conformations increases as the alkanes grow longer. For butane, the gauche conformation is about 4.0 kJ/mol less stable as compared with trans (anti) *n*-butane,<sup>18</sup> and at 25°C about 15% of the molecules will be in the gauche conformation. To test the accuracy of our single-conformation model, the vibrational profiles of trans and gauche butane were combined with weights according to the Boltzmann distribution. This resulted in only minute changes in the overall accuracy of the fit and an unchanged intramolecular shift in ionization energy.

## 4. Results and Discussion

**4.1. Experimental Spectra and Chemical Shifts.** The experimental spectra in Figure 1 reveal ionization energies that decrease with the length of the alkane, irrespective of whether the leading edge or the centroid of each spectrum is considered. At the same time, the vibrational features that are so dominating in the spectra of methane and ethane become less distinct in the longer chains because of chemically shifted subspectra. The rich vibrational structures are remarkably well fit by the theoretical profiles included as solid lines in Figure 1, with the underlying site-specific vibrational profiles drawn with finer lines. This warrants the high accuracy of the site-specific shifts in adiabatic ionization energies ( $\Delta I$ ) given in Table 1, with  $\Delta I$ 's given relative to an adiabatic ionization energy of 290.703 eV for methane.

**Table 1.** Site-Specific Shifts<sup>a</sup> in Adiabatic Ionization Energies ( $\Delta I$ , Relative to  $I = 290.703$  eV for Methane) for the *n*-Alkanes (eV)

	C1 <sup>b</sup>	C2	C3	C4
C <sub>2</sub> H <sub>6</sub> <sup>c</sup>	-0.158			
C <sub>3</sub> H <sub>8</sub>	-0.344	-0.216		
C <sub>4</sub> H <sub>10</sub>	-0.423	-0.377		
C <sub>5</sub> H <sub>12</sub>	-0.463	-0.421	-0.565	
C <sub>6</sub> H <sub>14</sub>	-0.486	-0.443	-0.616	
C <sub>8</sub> H <sub>16</sub>	-0.506	-0.457	-0.626	-0.709

<sup>a</sup> Estimated relative uncertainty 0.02 eV. <sup>b</sup> C1 denotes terminal carbon atoms. <sup>c</sup> From ref 2.

**Table 2.** Calculated Site-Specific Shifts<sup>a</sup> in Initial-State Energy ( $\Delta V$ , Relative to CH<sub>4</sub>) for the *n*-Alkanes (eV)

	C1 <sup>b</sup>	C2	C3	C4
C <sub>2</sub> H <sub>6</sub>	0.12			
C <sub>3</sub> H <sub>8</sub>	0.07	0.30		
C <sub>4</sub> H <sub>10</sub>	0.07	0.23		
C <sub>5</sub> H <sub>12</sub>	0.07	0.24	0.17	
C <sub>6</sub> H <sub>14</sub>	0.07	0.24	0.17	
C <sub>8</sub> H <sub>16</sub>	0.07	0.24	0.17	0.18

<sup>a</sup> Estimated relative uncertainty 0.02 eV. <sup>b</sup> C1 denotes terminal carbon atoms.

Within each *n*-alkane, the ionization energy drops from the end toward the center of the chain, cf. Figure 2. Numbering the carbon atoms according to their position from the end of the chain, we found that C2 forms an exception to this trend, in that C2 has a higher binding energy than that of C1. Decomposition of  $\Delta I$  into initial- and final-state contributions according to  $\Delta I = \Delta V - \Delta R$  shows that the relaxation term ( $\Delta R$ ) is responsible for the trend of lower ionization energies toward the center of each chain. The high ionization energy for C2 may, on the other hand, be attributed to the potential term as  $\Delta V$  shows an oscillatory behavior with the highest value for C2.

When comparing different *n*-alkanes, the relaxation energy is seen to increase with the length of the chain and to be responsible for the observed decrease in ionization energy with molecular size.

**4.2. Analysis of  $\Delta I$  in Terms of Group Electronegativity and Polarizability.** In this section, we link the computed trends in  $\Delta V$  and  $\Delta R$  to the concepts of electronegativity and polarizability, respectively, and thus gain insight into the chemical origin of the observed trends in the ionization energies.

We start out by looking at the shift in initial-state potential,  $\Delta V$ , as it appears from Table 2 and Figure 2. The dominating feature is that the potential increases with the number of alkyl groups directly attached to the ionized carbon; that is, the electrostatic potential of a methylene carbon is higher than that of a methyl carbon, which in turn is higher than the potential of carbon in methane. This finding may be understood with reference to the documented difference in group electronegativity between hydrogen and alkyls.<sup>19</sup> To a first approximation, every CH<sub>x</sub> moiety in a saturated hydrocarbon constitutes a neutral entity, with all hydrogens carrying the same net charge,  $q_H > 0$ . This model predicts the net charge on the carbon to be ionized as  $-4q_H$ ,  $-3q_H$ , and  $-2q_H$  for methane, methyl, and methylene, respectively, in good agreement with net charges from Mulliken population analysis:  $q_C = -0.51e$ ,

(16) van der Straten, P.; Morgenstern, R.; Niehaus, A. *Z. Phys. D* **1988**, *8*, 35.  
 (17) Rye, R. R.; Jennison, D. R.; Houston, J. E. *J. Chem. Phys.* **1980**, *73*, 4867.  
 (18) Verma, A.; Murphy, W.; Bernstein, H. *J. Chem. Phys.* **1974**, *60*, 1540.

(19) Bergmann, D.; Hinze, J. In *Structure and Bonding*; Sen, K. D., Jørgensen, C. K., Eds.; Springer-Verlag: Berlin, 1987; Vol. 66, pp 145–190.

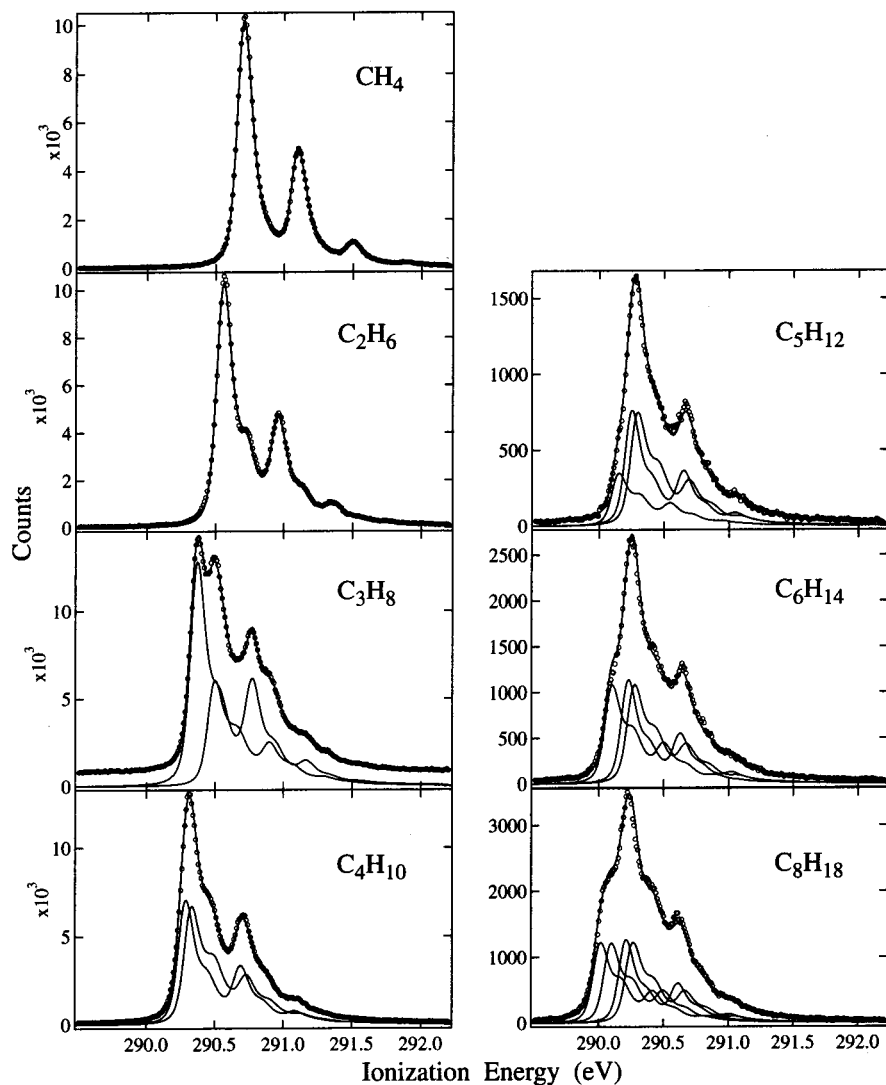


**Figure 1.** Experimental (O) and theoretical (—) C1s photoelectron spectra of CH<sub>4</sub>, C<sub>2</sub>H<sub>6</sub>,<sup>2</sup> C<sub>3</sub>H<sub>8</sub>, C<sub>4</sub>H<sub>10</sub>, C<sub>5</sub>H<sub>12</sub>, C<sub>6</sub>H<sub>14</sub>, and C<sub>8</sub>H<sub>18</sub>. The individual vibrational profiles for each site of ionization are also shown.

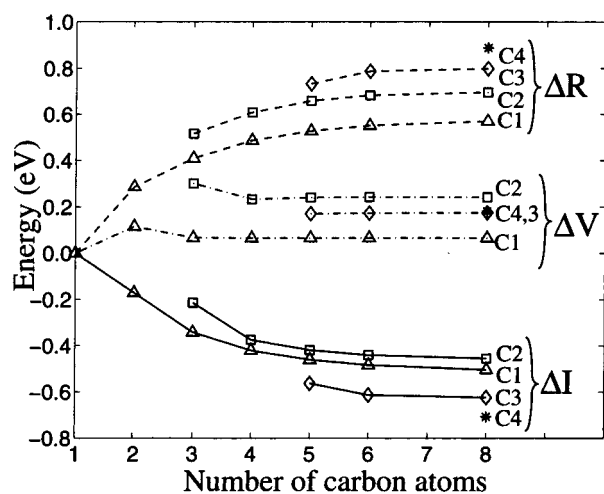


**Figure 2.**  $\Delta I$  as analyzed in terms of  $\Delta R$  and  $\Delta V$  contributions for each symmetry-unique carbon atom in the low-to-medium length alkanes.

$-(0.35-0.38)e$ , and  $-(0.20-0.25)e$  for carbon in CH<sub>4</sub>, CH<sub>3</sub>, and CH<sub>2</sub> moieties, respectively. The sequence  $0 < \Delta V_{C1} < \Delta V_{C \geq 2}$  then follows from the net atomic charge on carbon by reference to the potential model.<sup>20</sup>

At the more detailed level, when comparing two carbon atoms that have the same number of alkyl substituents, the potential is seen to increase with the number of methyl substituents. An example is the higher potential in ethane as compared to terminal carbon atoms in the longer hydrocarbons. The electronegativity of an alkyl substituent is often considered to increase with its length,<sup>19</sup> and, combined with the potential model, this would lead to a trend opposite to what is computed here. However, electronegativity reflects the typical or average ability of a functional group to withdraw electrons when engaged in a molecule. There is considerable evidence that methyl acts as an electron acceptor when bonded to a saturated moiety. Taking propane as an example, both theory and experiment show that the methyl moieties constitute the negative part of the molecule.<sup>7,21,22</sup> Partitioning the molecule into a methyl and an ethyl group, the ethyl part is then positively charged, contrary to expectations based on group electronegativity.<sup>19</sup> In the present context, methyl substituents withdraw electrons and thus act to increase the net charge and hence the potential at the site of

(20) Maksić, Z. B. In *Theoretical Models of Chemical Bonding*; Maksić, Z. B., Ed.; Springer-Verlag: Berlin, 1991; Vol. 3, p 289.

(21) Fort, R. C., Jr.; Schleyer, P. J. *Am. Chem. Soc.* **1964**, *86*, 4194.

(22) Muentner, J. S.; Laurie, V. W. *J. Chem. Phys.* **1966**, *45*, 855.

**Table 3.** Calculated Site-Specific Shifts<sup>a</sup> in Relaxation Energy ( $\Delta R$ , Relative to CH<sub>4</sub>) for the *n*-Alkanes (eV)

	C1 <sup>b</sup>	C2	C3	C4
C <sub>2</sub> H <sub>6</sub>	0.27			
C <sub>3</sub> H <sub>8</sub>	0.41	0.52		
C <sub>4</sub> H <sub>10</sub>	0.49	0.61		
C <sub>5</sub> H <sub>12</sub>	0.53	0.66	0.74	
C <sub>6</sub> H <sub>14</sub>	0.55	0.68	0.79	
C <sub>8</sub> H <sub>16</sub>	0.57	0.70	0.80	0.89

<sup>a</sup> Estimated relative uncertainty 0.03 eV. <sup>b</sup> C1 denotes terminal carbon atoms.

ionization. Interestingly, a similar increase in the initial-state potential is observed upon replacing one of the hydrogen atoms in H<sub>2</sub>S by CH<sub>3</sub>.<sup>23</sup> However,  $\Delta V$  decreases when proceeding to dimethyl sulfide, as it does when comparing hydrogenated to methylated electronegative moieties such as chlorine and the carboxyl group.<sup>23</sup> The situation is well summarized by Aitken et al.:<sup>24</sup> *Depending on the environment, alkyl groups act readily as either electron donors or electron acceptors.*

When considering how the potential varies within a single *n*-alkane, the discussed trends translate into  $0 < \Delta V_{C1} < \Delta V_{C\geq 3} < \Delta V_{C2}$ . This implies an oscillatory behavior from the end carbon atom toward the center of the chain, as confirmed in Table 2 for all the investigated *n*-alkanes. The oscillations are quickly attenuated toward the center of the chain.

Next, we turn to shifts in relaxation energies,  $\Delta R$ . According to Figure 2 and Table 3,  $\Delta R$  increases smoothly with increasing molecular size of the alkane. Moreover, considering different sites of ionization within a single *n*-alkane, the contribution from final-state relaxation to the ionization energy increases from the end toward the center of the molecule. Earlier studies<sup>4,25</sup> have shown that the difference in ionization energy and, more specifically, the difference in relaxation energy among *n*-alkanes are mainly determined by polarization effects. In the following, we aim to investigate whether this statement holds true also for site-specific ionization energies.

In general, final-state relaxation may be discussed in terms of intra- and extra-atomic contributions.<sup>4,5</sup> Intra-atomic relaxation is dominated by contraction of valence orbitals at the core-ionized atom ( $\Delta R^{\text{contr}}$ ) and depends on the net charge of the ionized atom. On the basis of the Mulliken charges listed above, we expect the intra-atomic relaxation to differ slightly between methane, methyl, and methylene carbon atoms, respectively, but not within each set. The extra-atomic relaxation energy is partly because of the flow of electrons from substituents to screen the core hole,  $\Delta R^{\text{flow}}$ , and partly because of polarization of the said substituents,  $\Delta R^{\text{pol}}$ . Following ionization, we found the valence Mulliken population to increase by 0.86–0.88 electrons for the ionized carbon at CH<sub>3</sub> sites, as compared to 0.90–0.97 electrons at CH<sub>2</sub> sites. These numbers suggest a small but systematic difference in  $\Delta R^{\text{flow}}$  between CH<sub>3</sub> and CH<sub>2</sub> carbon atoms. Moreover, whereas there is almost no variation in  $\Delta R^{\text{flow}}$  among methyl carbon atoms, there is some variation among methylene carbons.

To model polarization of substituents in the field from the ionized atom, we rely on an empirical representation of the

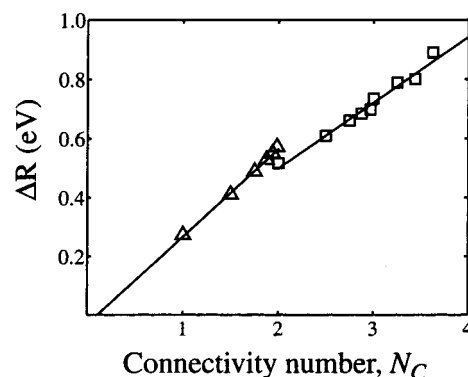


**Figure 3.** Site-specific shifts in electronic relaxation energy,  $\Delta R$ , relative to methane, plotted against the connectivity number for the CH<sub>2</sub> (□) and CH<sub>3</sub> (△) carbon atoms. Linear regression lines are included.

effective polarizability at a specific site. Gasteiger and Hutchings<sup>26</sup> demonstrated that for a molecule that is composed of equally polarizable sub-units, the polarization energy associated with a localized charge is linearly related to the connectivity number,  $N_c$ , which may be determined by a simple bond-counting procedure. Later, Nordfors and Ågren<sup>25</sup> extended this model to take into account units of different polarizability. In particular, they demonstrated that chemical shifts in C1s ionization energy among alkanes are linearly related to differences in the average connectivity number.

Taking only carbon–carbon bonds into account, the connectivity number pertaining to position *m* in an *n*-membered linear alkane is simply  $N_c = 2[2 - 2^{1-m} - 2^{m-n}]$ . The connectivity number associated with carbon–hydrogen bonds is given by  $4 + N_c/2$ . Shifts in relaxation energy relative to methane, for which  $N_c = 0$ , then become  $\Delta R^{\text{pol}} = (a_C + a_H/2)N_c$ . The constants  $a_C$  and  $a_H$  are related to the atomic polarizability of carbon and hydrogen, respectively. Taking also  $\Delta R^{\text{contr}}$  and  $\Delta R^{\text{flow}}$  into account, we found that the model needs to be generalized to

$$\Delta R = A + B \times N_c \quad (3)$$

where *A* and *B* are constants only for carbon sites that show the same value of  $\Delta R^{\text{contr}}$  and  $\Delta R^{\text{flow}}$ . On this background, the site-specific relaxation energies were grouped into two sets, pertaining to methylene and methyl carbon atoms, respectively, and plotted against  $N_c$  in Figure 3.  $\Delta R$  has a close-to-linear dependence on  $N_c$ , with correlation coefficients  $r^2 = 0.998$  and  $r^2 = 0.98$  for CH<sub>3</sub> and CH<sub>2</sub>, respectively. The lower correlation coefficients for the methylene set probably reflect the greater spread observed in the final-state Mulliken charges for these atoms. However, the important conclusion is that within each class of carbon atoms, the shift in relaxation energy is proportional to the connectivity number and thus the polarizability of the substituents.

**4.3. The Vibrationally Resolved Spectrum of Free Polyethylene.** One of the objects for measuring the spectra of the *n*-alkanes was to construct the spectrum of an isolated, extended strand of polyethylene by extrapolation. To the end of preparing such a reference spectrum, a set of vibrational profiles and corresponding ionization energies is needed.

(23) Siggel, M. R. F.; Thomas, T. D. *J. Am. Chem. Soc.* **1992**, *114*, 5795.

(24) Aitken, E. J.; Dahl, M. K.; Bomben, K. D.; Gimzewski, J. K.; Nolan, G. S.; Thomas, T. D. *J. Am. Chem. Soc.* **1980**, *102*, 4873.

(25) Nordfors, D.; Ågren, H. *J. Electron Spectrosc. Relat. Phenom.* **1991**, *56*, 1.

(26) Gasteiger, J.; Hutchings, M. G. *Tetrahedron Lett.* **1983**, *24*, 2537.

Of the molecules studied here, octane is expected to have line shapes most similar to those of the extended polymer. To investigate the convergence of the vibrational profiles, the spectrum of octane was fit using line shapes calculated for the smaller alkanes. The quality of the fits indicates that the C1 line shape of butane, C2 line shape from pentane, and C3 line shape from hexane are essentially equal to the line shapes computed for octane. This shows that the site-specific line shapes in octane are converged with respect to molecular size. Thus, three neighboring carbon atoms on one side of the ionization site seem to be sufficient for converging the vibrational profile. Furthermore, the C3 and C4 line shapes of octane are essentially equal, indicating inward convergence and that the line shapes of bulk atoms may be expected to be well described using either of these. On the basis of these observations, the site-specific line shapes of octane were used in the extrapolation scheme, and vibrational profiles of the bulk carbon atoms of the free polymer were represented by the C4 profile.

Ionization energies may be obtained from extrapolated values for  $\Delta V$  and  $\Delta R$ , combined according to eq 1. When extrapolating the site-specific values for  $\Delta V$  given in Table 2,<sup>27</sup> we obtain asymptotic values for each of the C1–C4 sites that are essentially identical to the corresponding values for octane. Hence, the latter were used for C1–C4 sites in the extended polymer. To obtain initial-state shifts for carbon atoms farther from the end, a second extrapolation was carried out, this time in the carbon position and on the basis of the C1–C4 values for octane. The resulting value of  $\Delta V = 0.18$  eV was used for the bulk carbon atoms in polyethylene. Turning to the relaxation term, we are in position to exploit the linear relationships between  $\Delta R$  and the connectivity number  $N_c$ , detailed in the preceding section. For an infinitely long strand of polyethylene, the relevant shift in relaxation energy is found from Figure 3 as  $\Delta R = 0.95$  eV (using  $N_c = 4$  for an infinitely long chain).

The spectra of  $C_7H_{16}$ ,  $C_8H_{18}$ ,  $C_{20}H_{42}$ , and  $C_{1000}H_{2002}$ , as presented in Figure 4, were generated by the interpolation/extrapolation scheme just outlined. The experimental spectrum of octane is included for comparison, and the deviations between the experimental and the synthetic spectrum illustrate the uncertainties to be expected in the extrapolated relaxation energies. The spectrum of heptane has not been measured and was therefore synthesized, showing great resemblance to the spectra of hexane and octane.

Turning to the model polymer spectrum on the bottom of Figure 4, we found that the general features are as expected from inspection of the spectra of the small alkanes. The low energy features are amplified, as previously seen in Figure 1, when going from pentane to octane and dominate the spectrum of the gas-phase extended polymer. The terminal carbon atoms have a notably higher binding energy than that of the interior atoms. This is manifested in the intermediate spectrum of  $C_{20}H_{42}$  showing significant broadening on account of contributions from the carbon atoms close to the end of the chain. The spectrum of the extended polymer is completely dominated by carbon atoms in the deep interior of the chain, and therefore chemical shift does not act as a source of broadening in this case.

The spectrum of free polyethylene puts us in a position to address the question of vibrational structures in the polymer.

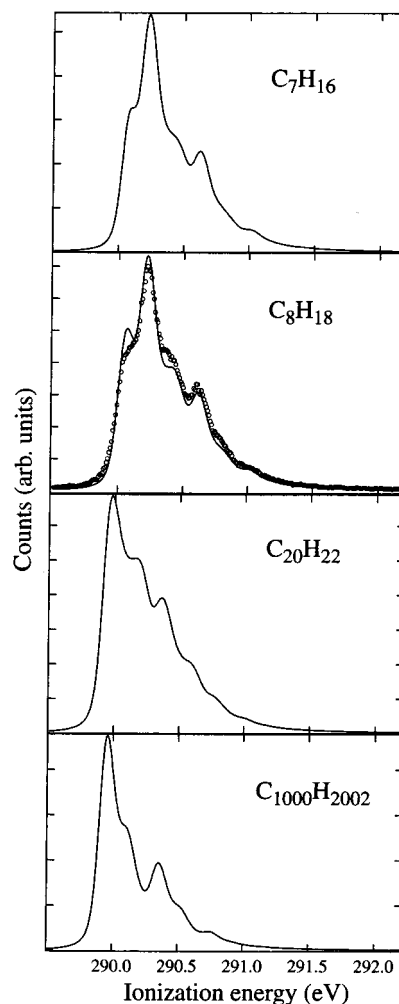


**Figure 4.** Extrapolated C1s spectra of  $C_7H_{16}$ ,  $C_8H_{18}$ ,  $C_{20}H_{42}$ , and  $C_{1000}H_{2002}$ . The experimental spectrum of octane is included (O) for comparison.

The vibrational structure of the single-molecule polymer is dominated by C–H stretching modes of the bulk atoms. This explains the success of a previous assignment of the solid-phase spectrum of polyethylene,<sup>9</sup> based on a vibrationally resolved gas-phase spectrum of methane.<sup>10</sup> In addition to C–H stretch, there are several low-energy modes being excited, corresponding to CCH and CCC bending and C–C stretching modes. Excitation of CCH bending modes is the origin of the shoulder on the high-energy side of the main peak. Adding a vibrational energy of 0.20 eV (vide supra) to the asymptotic adiabatic ionization energy (289.93 eV) leads to a value of 290.13 eV for the vertical ionization energy of an infinitely long strand of polyethylene.

Finally, to facilitate a comparison between our synthetic spectrum and an experimental XPS spectrum of solid-state polyethylene,<sup>9</sup> a less-resolved spectrum with postcollision effects neglected was prepared. Mainly because of differences in work function between the solid and gaseous phase, the ionization energy is significantly lower in the solid than in the gas phase. To circumvent this problem, the energy, as well as the intensity and Gaussian broadening (0.65 eV), of the free-molecule spectrum was determined in a fit to the spectrum in ref 9. From Figure 5, the agreement between our synthetic spectrum and the experimental, solid-state spectrum is very good.

(27) Bender, C. M.; Orszag, S. A. *Advanced Mathematical Methods for Scientists and Engineers*; McGraw-Hill: Singapore, 1984; pp 369–370.

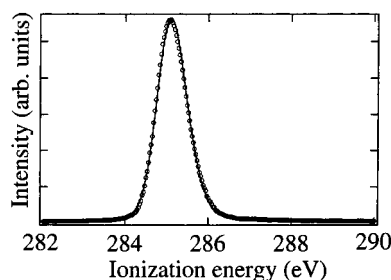


**Figure 5.** Carbon 1s photoelectron spectrum of solid-state polyethylene<sup>9</sup> (O) as fit by a broadened free-molecule spectrum of C<sub>1000</sub>H<sub>2002</sub> (–).

## 5. Conclusions

The excellent agreement between theoretical line shapes and our experimental spectra demonstrates the accuracy and advantages of using ab initio calculations for analyzing C1s spectra.

The carbon 1s ionization energies of the *n*-alkanes generally decrease with molecular size and inward in each chain. The outermost methylene carbon atom, C2, displays an exception to the latter trend, in that it consistently shows the highest ionization energy in the molecule. The reason for this is the electron-withdrawing ability of its methyl substituent, which leaves C2 at a high initial-state potential.

Observed shifts in C1s ionization energy are strongly correlated to the electronegativity (via the initial-state contribution,  $\Delta V$ ) and polarizability (via final-state relaxation,  $\Delta R$ ) of the alkyl groups. In particular,  $\Delta R$  turns out more important than  $\Delta V$  in these molecules, and shifts in C1s ionization energies are therefore mainly determined by the polarizability of the alkyl substituents.

From the synthetic spectrum of an extended, linear alkane, the vibrational structure in the carbon 1s spectrum of polyethylene is found to be dominated by C–H stretching modes, with additional contributions from CCH and CCC bending and C–C stretching modes.

**Acknowledgment.** This work has been supported by the Nordic Academy of Advanced Study, the Swedish Research Council for Natural Sciences (NFR), the Research Council of Norway (both financially and by grants of computing time), Göran Gustafsson's foundation, and Knut and Alice Wallenberg's foundation (KAW).

## Appendix: Computational Details

Equilibrium geometries, harmonic vibrational frequencies, and normal mode vectors were calculated by the hybrid density-functional theory method B3LYP<sup>28</sup> as implemented<sup>29</sup> in the Gaussian 98 set of programs.<sup>30</sup> In this functional, exchange effects are modeled both by explicit Hartree–Fock exchange

and by effective local and nonlocal density functionals. All calculations use atom-centered Gaussian-type functions contracted to triple- $\zeta$  quality<sup>31</sup> and augmented by polarization functions,<sup>32</sup> leading to C [5s, 3p, 1d] and H [3s, 1p]. For the core-ionized atom, the corresponding nitrogen basis was used with all exponents scaled by a common factor of 0.9293, obtained by minimizing the energy of core-ionized methane. The core of the ionized carbon atom was represented by Stevens and co-workers' effective core potential (ECP),<sup>33</sup> scaled to account for only one electron in the 1s shell.<sup>1</sup>

Ionization of C1s levels is accompanied by vibrational excitations, and the intensity of each vibrational line was computed<sup>34</sup> according to the Franck–Condon principle.<sup>14</sup> The present level of theory exaggerates the contraction in C–H bonds that takes place during ionization, by 0.3 pm as judged from very accurate calculations for methane<sup>1</sup> and ethane.<sup>2</sup> Hence, when computing Franck–Condon factors, C–H bonds at the ionized carbon atoms were lengthened accordingly.

Harmonic frequencies are calculated slightly too high as compared with experimental frequencies.<sup>2,13,35</sup> The vibrational energies were therefore scaled by a factor of 0.99, except for the symmetric C–H stretching mode on the core-ionized carbon atom which was scaled by 0.95. Furthermore, the symmetric C–H stretching mode at the core-ionized carbon atom was described as a Morse oscillator, with the anharmonicity constant ( $X_{11}$ ) taken from methane.<sup>1</sup> A more detailed account is given in ref 2 for the case of ethane.

As an approximation, we have considered the C1s orbitals to be fully localized to individual atoms. While this works well for the smaller alkanes,<sup>2</sup> with increasing chain length, core orbitals in the interior tend to interact and form a very narrow, inner-shell band structure. According to first-order degenerate perturbation theory,<sup>36,37</sup> the energy distribution of delocalized, coupled hole states in their vibrational ground states is given by

$$E_r = E_{\text{loc}} + 2\beta S^{(0,0)} \cos \frac{r\pi}{n+1}, \quad r = 1, 2, \dots, n \quad (4)$$

Here,  $E_r$  is the energy of level  $r$ ,  $E_{\text{loc}}$  is the energy of a localized hole state,  $\beta$  is the electronic coupling integral between final states having the core hole localized to neighboring carbon atoms, respectively, and  $S^{(0,0)}$  is the overlap integral between the associated vibrational functions (all  $\nu = 0$ ). The latter was calculated as suggested by Malmqvist and Forsberg<sup>38</sup> and found to decrease with increasing molecular size: 0.39 in octane as compared with 0.58 for ethane. By extrapolation,<sup>39</sup>  $S^{(0,0)} \approx 0.29$  in an infinitely extended polymer. Orbital energies for the short

(28) Becke, A. D. *J. Chem. Phys.* **1993**, *98*, 5648.

(29) Stevens, P. J.; Devlin, F. J.; Chablowski, C. F.; Frisch, M. J. **1994**, *98*, 11623.

(30) Frisch, M. J.; Trucks, G. W.; Schlegel, H. B.; Scuseria, G. E.; Robb, M. A.; Cheeseman, J. R.; Zakrzewski, V. G.; Montgomery, J. A., Jr.; Stratmann, R. E.; Burant, J. C.; Dapprich, S.; Millam, J. M.; Daniels, A. D.; Kudin, K. N.; Strain, M. C.; Farkas, O.; Tomasi, J.; Barone, V.; Cossi, M.; Cammi, R.; Mennucci, B.; Pomelli, C.; Adamo, C.; Clifford, S.; Ochterski, J.; Petersson, G. A.; Ayala, P. Y.; Cui, Q.; Morokuma, K.; Malick, D. K.; Rabuck, A. D.; Raghavachari, K.; Foresman, J. B.; Cioslowski, J.; Ortiz, J. V.; Baboul, A. G.; Stefanov, B. B.; Liu, G.; Liashenko, A.; Piskorz, P.; Komaromi, I.; Gomperts, R.; Martin, R. L.; Fox, D. J.; Keith, T.; Al-Laham, M. A.; Peng, C. Y.; Nanayakkara, A.; Challacombe, M.; Gill, P. M. W.; Johnson, B. G.; Chen, W.; Wong, M. W.; Andres, J. L.; Gonzalez, C.; Head-Gordon, M.; Replogle, E. S.; Pople, J. A. *Gaussian 98*, revision A.9; Gaussian, Inc.: Pittsburgh, PA, 1998.

(31) Dunning, T. H., Jr. *J. Chem. Phys.* **1971**, *55*, 716.

(32) Raghavachari, K.; Binkley, J. S.; Seeger, R.; Pople, J. A. *J. Chem. Phys.* **1980**, *72*, 650.

(33) Stevens, W. J.; Basch, H.; Krauss, M. J. *J. Chem. Phys.* **1984**, *81*, 6026.

(34) Børve, K. J. *g2fc*; University of Bergen, 2000.

(35) Shimanouchi, T. In *NIST Chemistry WebBook, NIST Standard Reference Database* (<http://webbook.nist.gov>); Mallard, W. G., Linstrom, P. J., Eds.; National Institute of Standards and Technology: Gaithersburg, MD, February 2000; Vol. 69.

(36) Murrell, J. N.; Kettle, S. F. A.; Tedder, J. M. *The Chemical Bond*, 2nd ed.; John Wiley: New York, 1992; p 181.

(37) Børve, K. J.; Sæthre, L. J.; Thomas, T. D.; Carroll, T. X.; Berrah, N.; Bozek, J. D.; Kukuk, E. *Phys. Rev. A* **2001**, *63*, 012506.

(38) Malmqvist, P.-Å.; Forsberg, N. *Chem. Phys.* **1998**, *228*, 227.

(39)  $S^{(0,0)}$  was extrapolated from data for short-chain *n*-alkanes, using a second-order polynomial in  $1/n$ ,  $n$  being the number of carbon atoms in the molecule.

*n*-alkanes indicate a constant  $2\beta$  of 0.016 eV, increasing to 0.023 eV when final-state relaxation is taken into account.<sup>2</sup> The decrease in  $S^{(0,0)}$  is offset by an increasing number of interacting states as the number of carbon atoms increases, leading to a narrow bandwidth of about 0.013 eV both for ethane and for

the extended polyethylene. In conclusion, interactions between localized core holes constitute a negligible source of line broadening in polyethylene.

JA010649J